

## Article

# Cationicity Enhancement on the Hydrophilic Face of Ctriporin Significantly Reduces Its Hemolytic Activity and Improves the Antimicrobial Activity against Antibiotic-Resistant ESKAPE Pathogens

Xudong Luo <sup>1</sup> , Huan Deng <sup>1</sup>, Li Ding <sup>2</sup>, Xiangdong Ye <sup>1</sup> , Fang Sun <sup>1</sup>, Chenhu Qin <sup>1</sup> and Zongyun Chen <sup>1,\*</sup>

<sup>1</sup> Institute of Biomedicine and Hubei Key Laboratory of Embryonic Stem Cell Research, College of Basic Medicine, Hubei University of Medicine, Shiyan 442000, China; luoxudong000@126.com (X.L.); dh15736090032@163.com (H.D.); yexiangdong7237@163.com (X.Y.); 2016202040055@whu.edu.cn (F.S.); 2016202040025@whu.edu.cn (C.Q.)

<sup>2</sup> Department of Clinical Laboratory, Dongfeng Hospital, Hubei University of Medicine, Shiyan 442000, China; dl2168@163.com

\* Correspondence: chenzy2005@hbm.u.edu.cn

**Abstract:** The ESKAPE pathogen-associated antimicrobial resistance is a global public health issue, and novel therapeutic strategies are urgently needed. The short cationic antimicrobial peptide (AMP) family represents an important subfamily of scorpion-derived AMPs, but high hemolysis and poor antimicrobial activity hinder their therapeutic application. Here, we recomposed the hydrophilic face of Ctriporin through lysine substitution. We observed non-linear correlations between the physicochemical properties of the peptides and their activities, and significant deviations regarding the changes of antimicrobial activities against different bacterial species, as well as hemolytic activity. Most importantly, we obtained two Ctriporin analogs, CM5 and CM6, these two have significantly reduced hemolytic activity and more potent antimicrobial activities against all tested antibiotic-resistant ESKAPE pathogens. Fluorescence experiments indicated they may perform the bactericidal function through a membrane-lytic action model. Our work sheds light on the potential of CM5 and CM6 in developing novel antimicrobials and gives clues for optimizing peptides from the short cationic AMP family.

**Keywords:** scorpion venom; short cationic antimicrobial peptide family; Ctriporin; peptide design; hemolytic activity; multidrug-resistant; ESKAPE

**Key Contribution:** We designed two low hemolytic anti-ESKAPE antimicrobial peptides from scorpion-venom-derived peptide Ctriporin belonging to the short cationic antimicrobial peptide family and provided new clues for peptide optimization of this sub-family.



**Citation:** Luo, X.; Deng, H.; Ding, L.; Ye, X.; Sun, F.; Qin, C.; Chen, Z. Cationicity Enhancement on the Hydrophilic Face of Ctriporin Significantly Reduces Its Hemolytic Activity and Improves the Antimicrobial Activity against Antibiotic-Resistant ESKAPE Pathogens. *Toxins* **2024**, *16*, 156. <https://doi.org/10.3390/toxins16030156>

Received: 21 November 2023

Revised: 3 March 2024

Accepted: 6 March 2024

Published: 18 March 2024



**Copyright:** © 2024 by the authors. Licensee MDPI, Basel, Switzerland. This article is an open access article distributed under the terms and conditions of the Creative Commons Attribution (CC BY) license (<https://creativecommons.org/licenses/by/4.0/>).

## 1. Introduction

Antibiotic resistance is an ever-increasing threat to public health around the world. Of the most importance, the ESKAPE pathogens, namely *Enterococcus faecium*, *Staphylococcus aureus*, *Klebsiella pneumoniae*, *Acinetobacter baumannii*, *Pseudomonas aeruginosa*, and *Enterobacter species*, have received the most significant concern [1–3]. In this context, there is an urgent need to develop novel antimicrobials to combat these pathogens.

Cationic  $\alpha$ -helical antimicrobial peptides (C $\alpha$ AMPs) have been largely identified from a wide range of organisms and reported to possess bactericidal activity against different kinds of pathogens [4–9]. C $\alpha$ AMPs are cationic amphiphilic molecules with a distinct hydrophilic face on which polar residues often position and a hydrophobic face where nonpolar residues often gather. Although the accurate mechanism for C $\alpha$ AMPs' bactericidal activity has yet to be determined, a proposed mechanism was reported that

C $\alpha$ AMPs could quickly kill the target bacterial cells through the formation of various kinds of lipophilic pores in the plasma membrane, resulting in metabolites leaking and finally cell death. Accordingly, C $\alpha$ AMPs exert their antimicrobial function with a significant reduction, although it may not be completely eliminated, of the probability of drug-resistant bacteria [10–13]. Therefore, C $\alpha$ AMPs represent one of the promising solutions for the treatment of antibiotic-resistant bacterial infections [14].

A wealth of C $\alpha$ AMPs have been identified from the venom glands of various scorpion species [4,9,15,16]. Among these peptides, the members of short cationic AMP family are a group of cationic  $\alpha$ -helical peptides with 17 to 19 residues, including Ctriporin [17], Mucroporin [18], Imcroporin [19], Stigmurin [20], TsAP-1 and TsAP-2 [21], AamAP1 and AamAP2 [22], and BmKb1 and BmKb2 [23]. Some peptides from this family were reported to show antimicrobial activity against methicillin-resistant *S. aureus* [17–20]. We identified Lausporin-2 from the venom of *Liocheles australasiae*, displaying antimicrobial activity against several species of methicillin-resistant staphylococci, including *S. aureus*, *S. epidermidis* and *S. capitis* [24]. In a recent study, we revealed a moderate antimicrobial activity of Ctriporin against carbapenem-resistant (CRE) *A. baumannii* [25]. However, two main issues hinder the medicinal application of the peptides from short cationic AMP family: i, the peptides of this family were not reported to be active against other members of ESKAPE pathogens; ii, they have poor antimicrobial activity and potent hemolytic activity as reported in the previous studies.

In the present study, we chosen scorpion peptide Ctriporin as a scaffold template, tested its antimicrobial potential against ESKAPE pathogens; to improve its anti-ESKAPE potency, we recomposed the hydrophilic face of Ctriporin by gradually increasing the number of lysine residues on this surface. We found that compared with the parent peptide Ctriporin, the antimicrobial activities of two Ctriporin analogs, that are CM5 and CM6, against antibiotic-resistant ESKAPE pathogens were significantly improved, while their hemolytic activities were significantly reduced. We observed non-linear correlations between the physicochemical properties of the peptides and their activities, and significant deviations regarding the changes of antimicrobial activities against different bacterial species, as well as their hemolytic activity. Mechanism studies suggested that the peptides may kill the bacteria through a membrane-lytic mode of action. Our study provided new molecules for drug development against ESKAPE pathogen infections; this study also provides insight into the optimization of other scorpion-derived C $\alpha$ AMPs, especially those of short cationic AMP family.

## 2. Results

### 2.1. Analogue Design of Ctriporin

Ctriporin is a 19-mer C $\alpha$ AMP identified from the scorpion *Chaerilus tricostatus* [17]. The HeliQuest server is an online platform that facilitates the analysis of the helix properties of a certain C $\alpha$ AMP [26]. First, we generated the helical wheel plot of the peptide using the HeliQuest server. As shown in Figure 1A, Ctriporin presents obvious amphiphilic characteristics in that most of the hydrophilic residues are located on one side (the hydrophilic face) and most of the hydrophobic residues on the other side (the hydrophobic face). To improve the antimicrobial potency of Ctriporin, we focused on the hydrophilic face of the peptide, and designed a series of analogs, namely CM1 to CM7, by gradually replacing the non-hydrophobic residues with lysine (K). Note that, since proline was shown to play a crucial role in determining C $\alpha$ AMP's performance [27], the proline at the seventh site of the peptide (Pro<sup>7</sup>) is the last residue to be replaced in our study. The sequences and the physicochemical parameters of Ctriporin and its analogs are shown in Table 1. With the increase of the number of lysine, the net charge of the peptide increases from +3 to +10, and the hydrophobic moment of the peptides increases gradually from 0.452 to 0.704, while the hydrophobicity of these peptides decreases gradually from 0.805 to 0.377. As can be seen in Figure S1, the increase of net charge on the hydrophilic face of Ctriporin induced a nearly linear changes of hydrophobicity and hydrophobic moment of the peptide,

indicating that the increase of net charge is a useful approach to change the hydrophobicity and hydrophobic moment of the peptide.

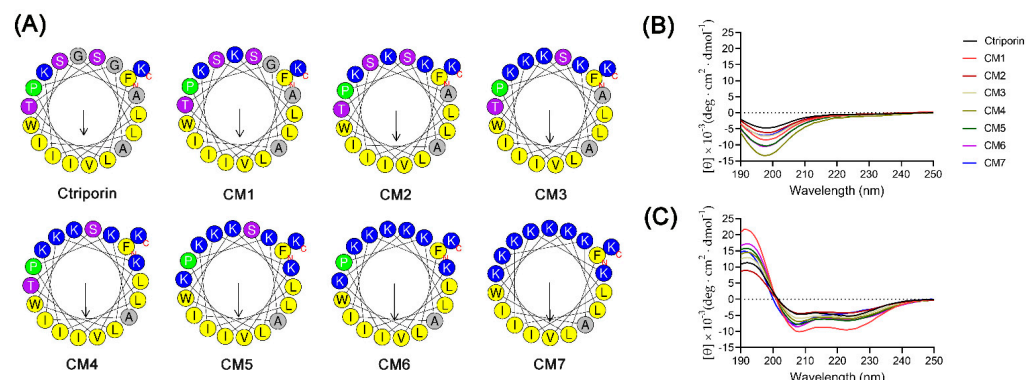


**Figure 1.** Structural analysis of Ctriporin and its analogs. **(A)** The helical wheel diagrams. The hydrophobic residues and lysine are presented in yellow and blue color, respectively. **(B,C)** CD spectra of Ctriporin and its analogs ( $150 \mu\text{g mL}^{-1}$ ) in ddH<sub>2</sub>O and 30 mM sodium dodecyl sulfate (SDS) solutions.

**Table 1.** Physicochemical parameters of Ctriporin and its analogs.

Peptide	Sequence <sup>a</sup>	aa <sup>b</sup>	MW <sup>c</sup>	z <sup>d</sup>	<H> <sup>e</sup>	< $\mu$ H> <sup>f</sup>
Ctriporin	FLWGLIPGAISAVTSLIKK	19	2013.5	3	0.805	0.452
CM1	FLWKLIPGAISAVTSLIKK	19	2084.6	4	0.753	0.503
CM2	FLWKLIPKAISAVTSLIKK	19	2155.7	5	0.701	0.547
CM3	FLWKLIPKAIKAVTSLIKK	19	2196.8	6	0.651	0.592
CM4	FLWKLIPKAIKKVTSLIKK	19	2253.9	7	0.583	0.614
CM5	FLWKLIPKAIKKVKSLIKK	19	2282.0	8	0.517	0.615
CM6	FLWKLIPKAIKKVKKLIKK	19	2323.1	9	0.467	0.664
CM7	FLWKLIPKAIKKVKKLIKK	19	2353.1	10	0.377	0.704

<sup>a</sup> All peptides are amidated at the C-terminus; <sup>b</sup> aa, amino acids; <sup>c</sup> MW, the molecular weights were determined with mass spectrometry; <sup>d</sup> z, the net charges were determined at pH 7.4; <sup>e</sup> <H>, the mean hydrophobicity; <sup>f</sup> < $\mu$ H>, the hydrophobic moments.

C $\alpha$ AMPs display  $\alpha$ -helical conformation in plasma membrane mimic environments. Therefore, the secondary structural contents of the peptides were measured using a circular dichroism (CD) Spectrometer. As shown in Figure 1B, the CD spectra of Ctriporin and its analogs exhibited a negative peak at a wavelength near 200 nm, indicating random coiled conformations of these peptides. However, as shown in Figure 1C, the CD spectra of Ctriporin and its analogs exhibited a positive peak at a wavelength near 195 nm and two negative peaks at 208 and 222 nm, indicating typical  $\alpha$ -helical conformations. Note, compared with other peptides, CM7 exhibited a significant different CD spectra as the intensity of the negative peak at 222 nm was significantly reduced, indicating that the substitution of Pro<sup>7</sup> may have impact on the secondary structure of this peptide in membrane mimic environment.

## 2.2. CM5 and CM6 Exhibited the Most Potent Antimicrobial Activity and the Lowest Hemolytic Activity

The ESKAPE pathogens represent the main threat to public health concerning antimicrobial resistance. Therefore, we first evaluated the antimicrobial activities of Ctriporin and its analogs against the standard ESKAPE strains. The minimum inhibitory concentration (MIC) was chosen as the index for the evaluation of each peptide's activity [28]. As shown in Table 2, the MICs of Ctriporin against *S. aureus* and *A. baumannii* were determined to be 16–32  $\mu\text{g/mL}$ , and for other tested bacterial species, these values were  $\geq 64 \mu\text{g/mL}$ . Compared with Ctriporin, increasing the number of lysine on the hydrophilic face has

a significantly positive effect on its antimicrobial activity. As can be seen, the MICs of CM3 and CM6 against these pathogens were determined to be 4–8  $\mu\text{g}/\text{mL}$  and those for CM5 were determined to be 2–8  $\mu\text{g}/\text{mL}$ . Note that the MICs of CM4 and CM7 are 4–32 and 8–32  $\mu\text{g}/\text{mL}$ , respectively, indicating the existence of significant bacterial species deviations for the antimicrobial activity of these peptides. In addition, the replacement of specific residues, especially Pro<sup>7</sup>, may harm the antimicrobial activities of the peptide. Taken together, CM3 (4–8  $\mu\text{g}/\text{mL}$ ), CM5 (2–8  $\mu\text{g}/\text{mL}$ ), and CM6 (4–8  $\mu\text{g}/\text{mL}$ ) are peptides showing the most potent activities against the ESKAPE pathogens and the smallest bacterial species deviation.

**Table 2.** Antimicrobial activities of Ctriporin and its analogs against standard strains.

	<i>S. aureus</i> ATCC29213	<i>S. aureus</i> ATCC25923	<i>E. faecium</i> ATCC29212	<i>E. coli</i> ATCC25922	<i>E. coli</i> ATCC35218	<i>P.</i> <i>aeruginosa</i> ATCC27853	<i>K.</i> <i>pneumoniae</i> ATCC700603	<i>A.</i> <i>baumannii</i> ATCC19606	
	MICs $\mu\text{g}/\text{mL}$ ( $\mu\text{M}$ )								Hemolysis% at 256 $\mu\text{g}/\text{mL}$
Ctriporin	16 (8.0)	32 (15.9)	64 (31.8)	64 (31.8)	>64 (31.8)	>64 (31.8)	>64 (31.8)	16 (8.0)	90.6 $\pm$ 11.8
CM1	8 (3.8)	16 (7.7)	16 (7.7)	8 (3.9)	32 (15.4)	>64 (30.7)	64 (30.7)	8 (3.8)	75.6 $\pm$ 10.1
CM2	4 (1.9)	8 (3.7)	4 (1.9)	4 (1.9)	8 (3.7)	16 (7.4)	16 (7.4)	4 (1.9)	74.3 $\pm$ 9.2
CM3	4 (1.8)	4 (1.8)	4 (1.8)	4 (1.8)	4 (1.8)	8 (3.6)	8 (3.6)	4 (1.8)	89.1 $\pm$ 12.1
CM4	4 (1.8)	8 (3.6)	16 (7.1)	8 (3.6)	16 (7.1)	16 (7.1)	32 (14.2)	4 (1.8)	14.0 $\pm$ 4.7
CM5	4 (1.8)	4 (1.8)	8 (3.5)	8 (3.5)	4 (1.8)	4 (1.8)	8 (3.5)	2 (0.9)	9.8 $\pm$ 0.6
CM6	8 (3.4)	8 (3.4)	8 (3.4)	8 (3.4)	8 (3.4)	4 (1.7)	8 (3.4)	4 (1.7)	8.1 $\pm$ 1.9
CM7	32 (13.6)	32 (13.6)	32 (13.6)	32 (13.6)	16 (6.8)	8 (3.4)	32 (6.8)	8 (3.4)	57.5 $\pm$ 9.8

Another purpose of this work is to attenuate Ctriporin's hemolytic activity. As shown in Figure 2, the curves of hemolysis% vs. peptide concentration of CM1, CM2, and CM3 are similar to that of Ctriporin. Interestingly, the percent hemolysis of CM4, CM5, and CM6 decreased dramatically compared with Ctriporin. Like antimicrobial activity, the replacement of Pro<sup>7</sup> harms hemolytic activity attenuation, as the curve of hemolysis% of CM7 positions closely to those of CM3. To better illustrate the difference in each peptide's hemolytic activity, the hemolysis% values of these peptides at 256  $\mu\text{g}/\text{mL}$  were summarized in Table 2. As can be seen, CM5 (9.8  $\pm$  0.6%) and CM6 (8.1  $\pm$  1.9%) are the two peptides with the lowest hemolytic activity. Although CM3 displays potent MICs (4–8  $\mu\text{g}/\text{mL}$ ), it also shows strong hemolytic activity. Therefore, CM5 and CM6 are the two Ctriporin analogs that exhibit the most potent antimicrobial activity and the lowest hemolytic activity.

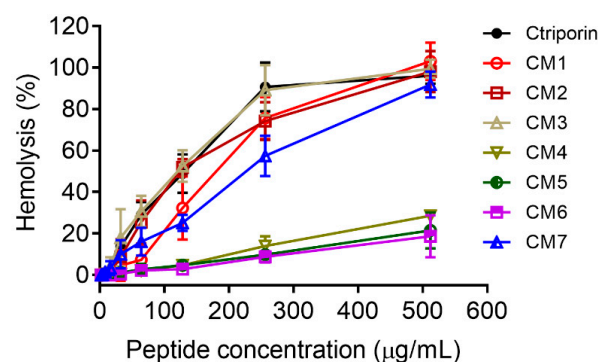


**Figure 2.** Hemolytic activities of Ctriporin and its analogs against human red blood cells (hRBC). Hemolytic activities of Ctriporin (solid circle), CM1 (open circle), CM2 (open square), CM3 (upward triangle), CM4 (downward triangle), CM5 (half solid circle), CM6 (half solid square), and CM7 (half solid triangle), were measured against 2% (*v/v*) human red blood cells. The peptide concentrations are 0, 2, 4, 8, 16, 32, 64, 128, 256, and 512  $\mu\text{g}/\text{mL}$ . The cells treated with 1% Triton X-100 were treated as 100% hemolysis. All experiments were repeated three times, and the data shown are the average  $\pm$  standard error.

### 2.3. The Correlations between the Physicochemical Properties and the Activities of Ctriporin and Its Analogs

The physicochemical properties, that are the net charge, the hydrophobicity, and the hydrophobic moment, are three critical parameters that affect C $\alpha$ AMPs' activities. However, the correlations between the physicochemical properties of C $\alpha$ AMPs and their antimicrobial or hemolytic activities are complicated and vary significantly between different C $\alpha$ AMPs [29]. In an attempt to provide clear profiles between these parameters and the activities of Ctriporin and its analogs investigated in this study, Figure 3 was generated through locally weighted regression fitting [30,31]. Generally, non-linear correlations were observed between physicochemical properties and the functions of these peptides. In terms of antimicrobial activity, bowl-shaped curves were obtained. In detail, as the net charges and the hydrophobic moments increase, and the hydrophobicity decreases from Ctriporin to CM5, either the values of MICs against *S. aureus* (Figure 3A–C) or the values against *A. baumannii* (Figure 3D–F) decrease rapidly, indicating the improvement of antimicrobial activities; however, further changes in the same directions led to increase of MICs, indicating the damage to antimicrobial activities. In addition, Figure 3A–F displays distinct sharps of *S. aureus* vs. *A. baumannii*, combining the results shown in Table 2, these results indicated significant variations in MICs between bacterial species.

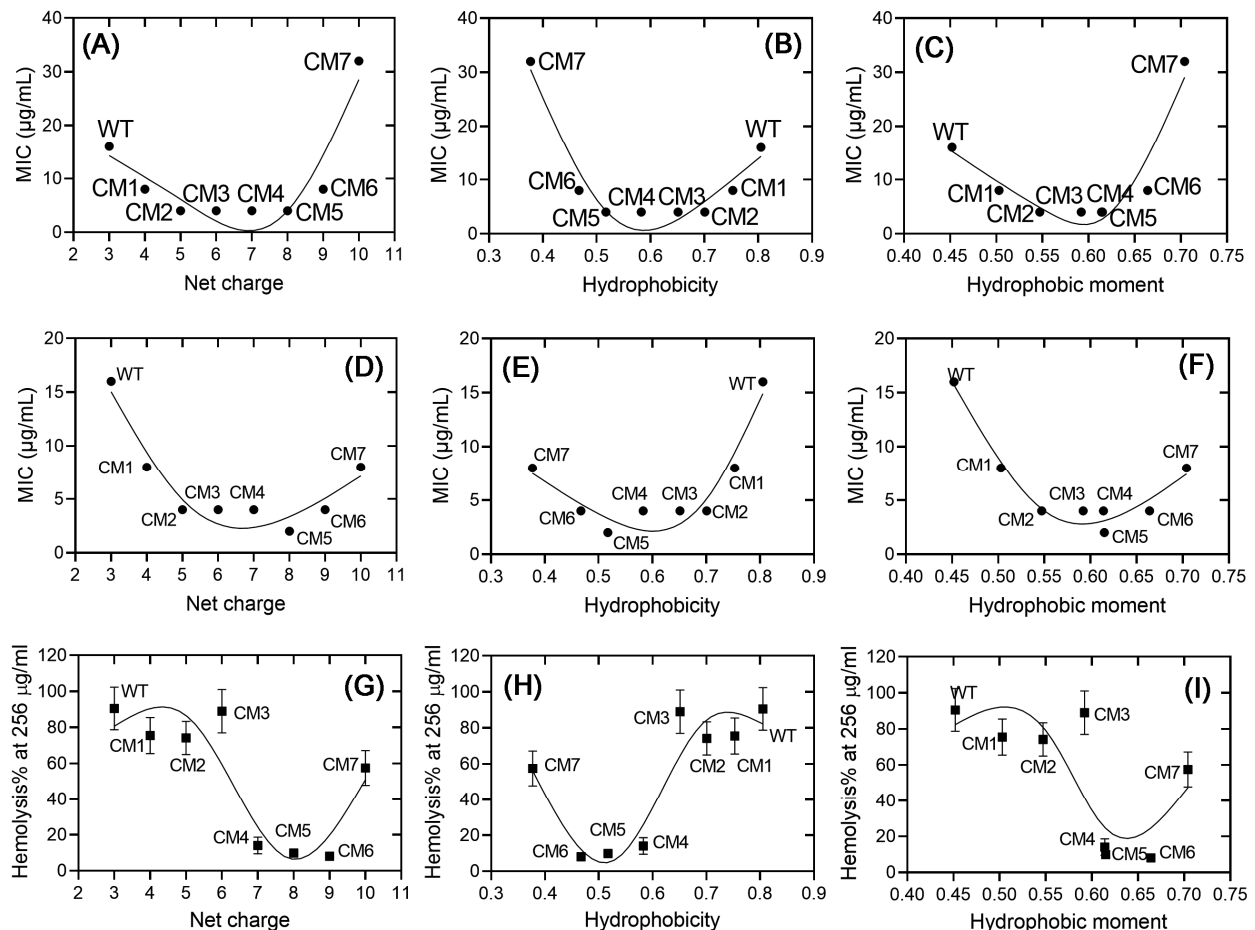


**Figure 3.** The correlations between the net charge (A,D,G), the hydrophobicity (B,E,H), the hydrophobic moment (C,F,I) of the peptides and their activities. (A–C): *S. aureus* ATCC29213; (D–F): *A. baumannii* ATCC19606; (G–I): hemolysis% of the peptides at 256  $\mu\text{g/mL}$ . Note, the hydrophobic moments of CM4 and CM5 are very close, the nodes are overlapped in (C). The error bar represents the standard variation of each value.

In terms of hemolytic activity, however, as shown in Figure 3G–I, curves with “Z” or “S” sharps were observed. No significant changes in hemolysis% were observed when the net charges increased from +3 to +6, the values of hydrophobicity decreased from 0.805 to 0.651, or the hydrophobic moments increased from 0.452 to 0.592. After that, the percentage of hemolysis decreased quickly; however, a significant increase in the percentage of hemolysis was observed in CM7. Taken together, our analysis suggested non-linear correlations between the physiochemical properties and the activities of Ctriporin and its analogs designed in this study, and significant variations between bacterial species, as well as hemolytic activity vs. antimicrobial activities.

#### 2.4. Antimicrobial Activities of CM5 and CM6 against Clinical Isolates of ESKAPE Pathogens

To further evaluate the antimicrobial potential of CM5 and CM6, the MICs of these two peptides, as well as the parent peptide Ctriporin, were determined against clinical antibiotic-resistant isolates of ESKAPE strains. As shown in Table 3, Ctriporin displayed poor antimicrobial activities against these strains, whereas those of CM5 and CM6 were significantly improved. In particular, CM5 and CM6 displayed MIC values of 2 µg/mL against clinical isolates of CRE and multidrug-resistant (MDR) *A. baumannii*. Note that CRE and MDR *A. baumannii* are listed at the top of the pathogens threatening public health [32]. Compared with the parent peptide Ctriporin, eight to sixteen times improvement in terms of antimicrobial activity was obtained through our peptide design strategy.

**Table 3.** Antimicrobial activities of Ctriporin, CM5 and CM6 against the clinical strains of the ESKAPE pathogens.

Strains	Resistance	Ctriporin	CM5	CM6
		MICs µg/mL (µM)		
<i>S. aureus</i> 9124	MRSA <sup>a</sup>	8 (4.0)	8 (3.5)	8 (3.4)
<i>S. aureus</i> 891	MRSA	16 (8.0)	4 (1.8)	8 (3.4)
<i>S. epidermidis</i> 6943	MRSE <sup>b</sup>	8 (4.0)	4 (1.8)	4 (1.7)
<i>S. epidermidis</i> 9092	MRSE	8 (4.0)	4 (1.8)	4 (1.7)
<i>S. capitis</i> 3255	MRSC <sup>c</sup>	8 (4.0)	2 (0.9)	2 (0.86)
<i>E. faecium</i> 898	MDR <sup>d</sup>	16 (8.0)	4 (1.8)	4 (1.7)
<i>E. coli</i> 2678	ESBL <sup>e</sup>	64 (31.8)	8 (3.5)	8 (3.4)
<i>E. coli</i> 2687	ESBL	>64 (31.8)	8 (3.5)	8 (3.4)
<i>P. aeruginosa</i> 9014	CRE <sup>f</sup> /MDR	>64 (31.8)	8 (3.5)	8 (3.4)
<i>K. pneumoniae</i> 9126	CRE	>64 (31.8)	16 (7.0)	16 (6.9)
<i>A. baumannii</i> 19295	CRE/MDR	32 (15.9)	2 (0.9)	2 (0.86)
<i>A. baumannii</i> 19462	CRE/MDR	16 (8.0)	2 (0.9)	2 (0.86)
<i>A. baumannii</i> 19618	CRE/MDR	32 (15.9)	2 (0.9)	2 (0.86)

<sup>a</sup> MRSA: methicillin-resistant *S. aureus*; <sup>b</sup> MRSE: methicillin-resistant *S. epidermidis*; <sup>c</sup> MRSC: methicillin-resistant *S. capitis*; <sup>d</sup> MDR: multidrug resistant; <sup>e</sup> ESBL: Extended-spectrum β-lactamases; <sup>f</sup> CRE: carbapenem-resistant.

#### 2.5. Growth Inhibitory Effects of CM5

To further confirm the antimicrobial activity of the peptides, CM5 was chosen and the growth inhibitory curves were measured against *A. baumannii* ATCC19606, and the clinical isolates 19295, 19618, and 19462. As shown in Figure 4, compared with the samples without treatment of CM5, the additions of 0.25 and 0.5 × MIC of the peptide have no inhibitory effects on the growth of the strains ATCC19606, and the clinical isolates 19295 and 19618. Still, the same dosages displayed some extent of inhibitory effects on the clinical isolates 19462. Interestingly, a similar phenomenon has been observed for the same strain in our previous study [25], this feature may imply some unique feature of this strain, or provide some clues as to the mechanism of action of the peptides, which deserves further investigation in future studies. Finally, the additions of 1, 2, and 4 × MIC of the peptide inhibited the growth of all tested strains, which is consistent with the results of MIC assays.

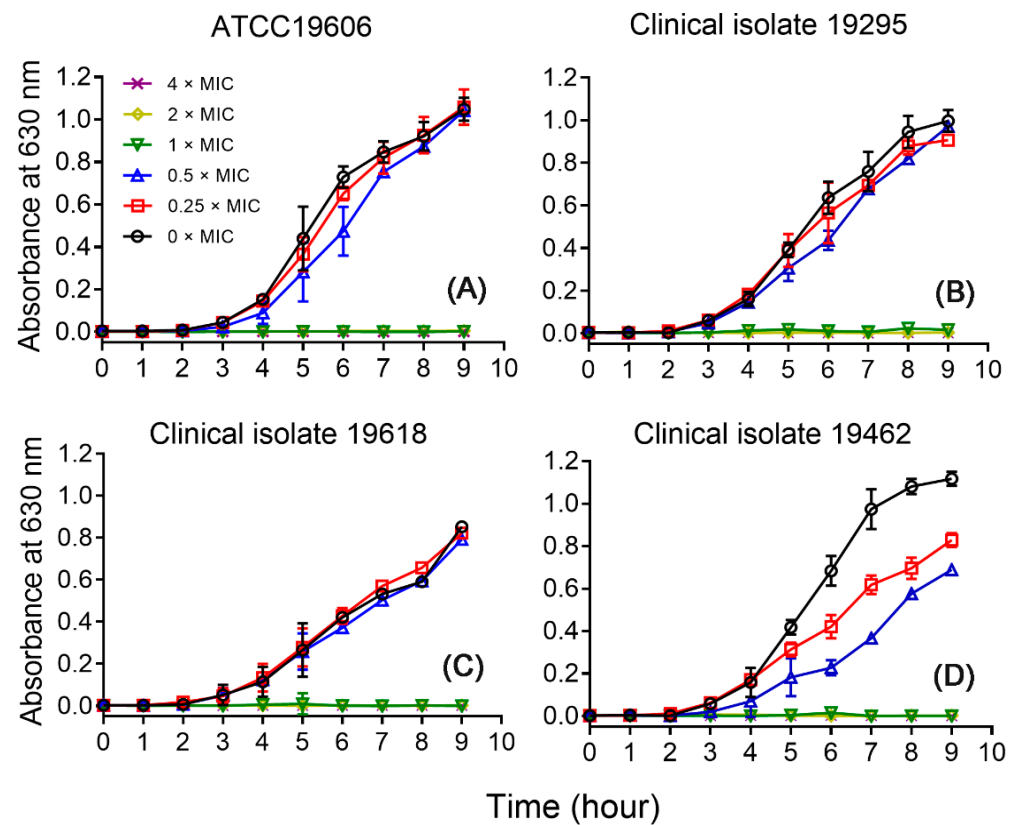


**Figure 4.** Time-growth curves of CM5 treated *A. baumannii* ATCC19606 (A), and the clinical isolates 19295 (B), 19618 (C), and 19462 (D). The peptide concentrations were 0 (open circle), 0.25 (open square), 0.5 (upward triangle), 1 (downward triangle), 2 (diamond), and 4 (cross) × MIC. The curves shown are the average  $\pm$  standard error of data derived from three independent experiments.

## 2.6. Bacterial-Killing Kinetics

To evaluate the bacterial-killing ability of CM5, *A. baumannii* ATCC19606 was chosen and the time-killing kinetics of the peptide against this bacterial strain was measured. As shown in Figure 5, a concentration-dependent decrease of viable bacterial cells was observed in a short time interval upon the addition of 1, 2, and 4 × MIC of the peptide. The results indicated that CM5 exhibits fast bactericidal activity.

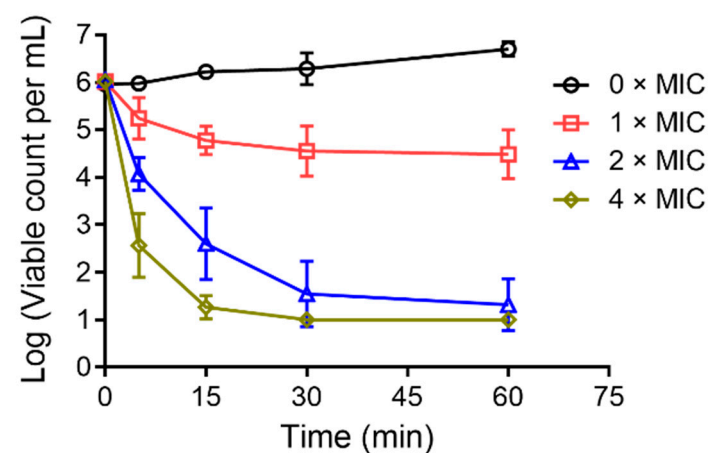


**Figure 5.** Time-killing kinetics of *A. baumannii* ATCC19606 treated with CM5. The bacterial cells were incubated without (open circle) or with 1 (open square), 2 (upward triangle), and 4 (diamond) × MIC peptides, respectively. The data shown are the means  $\pm$  SD of three independent experiments.

### 2.7. CM5 Induces Dose-Dependent Membrane Disruptions of the Bacterial Cells

It has been suggested that linear C $\alpha$ AMPs kill pathogens through pore formation in the plasma membrane of targeted bacterial cells, that is the so-called membrane-lytic mode of action [8,10]. PI is a classical DNA-binding probe that can permeate only compromised cell membranes [33]. It is a useful tool for the detection of membrane disruptions caused by C $\alpha$ AMPs. As shown in Figure 6A,B, the co-incubation of CM5 with *A. baumannii* ATCC19606 caused fast and dose-dependent PI fluorescence increase, indicating the addition of the peptide induced membrane disruption on the plasma membrane of the bacterial cells.

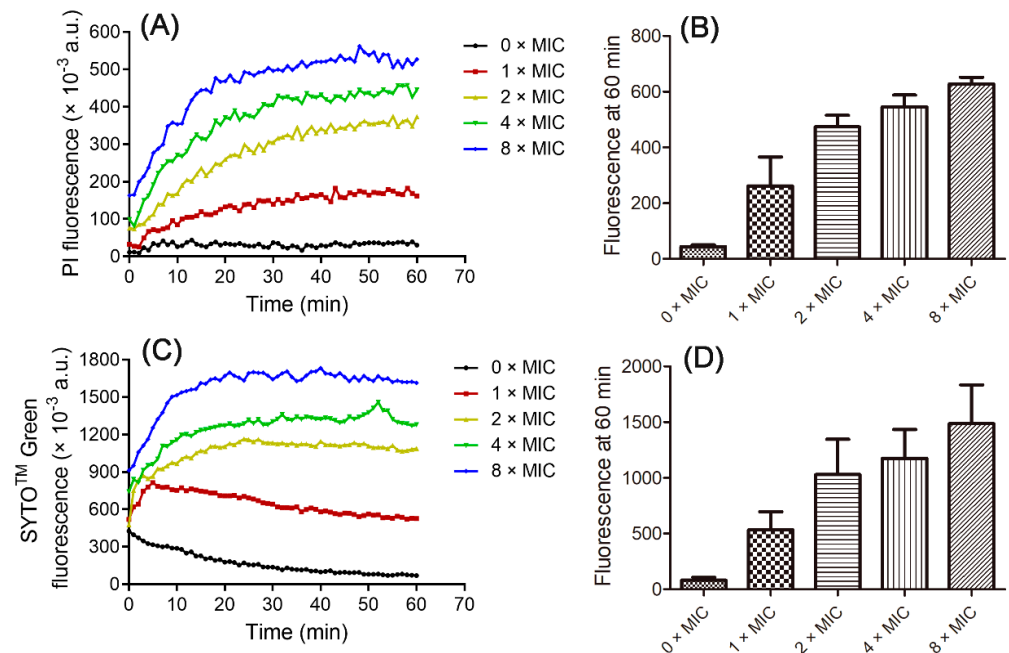


**Figure 6.** Membrane permeation of *A. baumannii* ATCC19606 treated with CM5. (A) PI fluorescence kinetics of the bacterial cells treated with the peptide; (B) PI fluorescence at 60 min; (C) SYTO<sup>TM</sup> Green fluorescence kinetics of the bacterial cells treated with the peptide. (D) SYTO<sup>TM</sup> Green fluorescence at 60 min. In (A,C), the bacterial cells incubated without (black) or with 1 (brown), 2 (yellow), 4 (green), and 8 (blue × MIC are shown, respectively. The data shown are the means ± SD of three independent experiments.

For further demonstration of this effect, the SYTO<sup>TM</sup> Green fluorescence assay was performed. SYTO<sup>TM</sup> Green is another DNA-binding probe displaying the same permeation mechanism as PI but with a different chemical structure and property, and was often used to illustrate membrane disruptions induced by antimicrobial peptides [34]. As shown in Figure 6C,D, a similar dose-dependent fluorescence increase was observed for the bacterial cells incubated with CM5. Taken together, the fluorescence assays, combined with time-killing kinetics assay, suggested that CM5 may perform a membrane-lytic mode of action.

### 3. Discussion

The ESKAPE pathogens exert a significant threat to public health. To fight against ESKAPE-caused antimicrobial resistance, the development of novel antimicrobials is of the most significance. Ctriporin is a highly hemolytic linear cationic antimicrobial peptide that has been demonstrated to be moderately active against bacteria *S. aureus* and *A. baumannii*, but poorly or inactive against other kinds of ESKAPE pathogens [15,25]. In this study, through cationicity enhancement on the hydrophilic face of the peptide by lysine substitution, we obtained CM5 and CM6, two Ctriporin analogs with significantly reduced hemolytic activity and much improved antimicrobial activities against all tested

ESKAPE strains. Our work provided new clues for the development of antimicrobials against infectious diseases caused by ESKAPE pathogens.

The high hemolytic activity and low antimicrobial activity represents the major disadvantages of natural C $\alpha$ AMPs. Natural C $\alpha$ AMPs are characterized by the relatively high occurrence frequency of alkaline residues such as lysine and arginine [35]. Although there are exceptions, in most cases, the alkaline residues are positioned on the hydrophilic surface of the peptides. These two kind of residues were used in several previous studies regarding natural CaAMPs in an attempt to reduce the hemolytic activity and improve their antimicrobial activities against different bacterial species [36–43]. However, due to the extreme diversity of sequence composition of these peptides, the above-mentioned strategies were largely based on empirical trial and error, and may not fit for other C $\alpha$ AMPs' optimization. In our previous studies, we demonstrated the improvement of the antimicrobial potency of 13-mer scorpion-derived C $\alpha$ AMP BmKn2 through cationicity enhancement, followed by replacing arginine with lysine on the hydrophilic face of the peptide, and designed BmK2-7K, a C $\alpha$ AMP composed of sole lysine on its hydrophilic face, displaying relative low hemolytic activity and potent antimicrobial activities against antibiotic-resistant ESKAPE pathogens [44,45]. To further investigate lysine replacements on the hemolytic and antimicrobial activities of natural peptides from another family of scorpion-derived C $\alpha$ AMP, we focused on the hydrophilic surface of scorpion-derived 19-mer peptide Ctriporin belonging to short cationic antimicrobial peptide family and found that increasing the number of lysine on this surface led to significant hemolysis attenuation and antimicrobial activity enhancement. Our studies indicated that lysine substitutions on the hydrophilic face may be a useful strategy for scorpion-derived short C $\alpha$ AMPs. However, this study revealed distinct optimal profiles for net charge adjustment of the peptides regarding different bacterial species. In addition, the optimal net charge range of the peptides regarding hemolytic activity was observed to be more narrow compared with that of antimicrobial activities in most cases. These results indicated the difficulty when designing low-toxic broad-spectrum antimicrobial peptides. Finally, unlike 13-mer C $\alpha$ AMP BmKn2, excessive increases of lysine were harmful to Ctriporin analogs. This phenomenon was also observed in the previous study [46], however, in our case, is this result caused by proline mutation which led to significant structural change in the peptide, as evidenced by our CD spectra profile needs further investigation.

To date, several groups of scorpion-derived C $\alpha$ AMPs have been identified so far from many different scorpion species [4]. However, the previous investigations were mostly focused on the identification and optimization of short peptides (i.e., 13–14 amino acids) [42,43,45,47–50], and the therapeutic potential of peptides of short cationic antimicrobial peptide family was largely overlooked due to their high hemolytic activity and poor antimicrobial activity. We for the first time performed a structure-activity relationship investigation on Ctriporin and obtained two analogs, CM5 and CM6. They were demonstrated to display much lowered hemolytic activity and much better antimicrobial activities against antibiotic-resistant ESKAPE pathogens. Our study sheds light on the therapeutical potential of the members of the short cationic antimicrobial peptide family and provides clues for the optimization of these peptides.

## 4. Materials and Methods

### 4.1. Peptide Analysis and Synthesis

All peptides used in this study were synthesized using solid-phase methods by Sangon Biotech (Shanghai, China) and amidated at the C-terminus of the peptides. The purities of the peptides (>95%) were analyzed by reversed-phase high-performance liquid chromatography [51]. The molecular weights of the peptides were measured by mass spectrometry. The helical-wheel plots, net charges, mean hydrophobicity values, and hydrophobic moments of the peptides were obtained using the HeliQuest server (<https://heliquest.ipmc.cnrs.fr/>, accessed on 5 March 2024) [24,26].

#### 4.2. Circular Dichroism

The secondary structural contents of the peptides were measured at 25 °C using a circular dichroism spectrometer (Chirascan plus, Applied Photophysics, Charlotte, NC, USA). A quartz cell with a 0.1 cm light path was employed in the experiments. Peptides were dissolved in either distilled H<sub>2</sub>O or 30 mM sodium dodecyl sulfate (Sigma-Aldrich, St. Louis, MO, USA) solutions to achieve a concentration of 150 µg mL<sup>-1</sup>. Three scans of the CD spectra (λ<sub>190–250</sub> nm) were obtained for each sample. The mean residue molar ellipticity was calculated from the original CD data by the equation, as described in the previous study [44]. The results are the average ± standard error of data derived from three independent experiments.

#### 4.3. Bacterial Strains

The standard strains, including *S. aureus* ATCC29213 and ATCC25923, *E. faecalis* ATCC29212, *E. coli* ATCC25922 and ATCC35218, *A. baumannii* ATCC19606, *K. pneumoniae* ATCC700603, and *P. aeruginosa* ATCC27853, were purchased from the China Center of Type Culture Collection (CCTCC). The clinical strains of the ESKAPE pathogens were isolated from the affiliated hospitals of Hubei University of Medicine [24,25,44]. All of them were stored at −80 °C before use. The drug sensitivities of the clinical strains were determined by the Kirby–Bauer test [52].

#### 4.4. Minimum Inhibitory Concentration (MIC) Determination

The MICs were determined using the broth dilution method according to the guidelines of the Clinical and Laboratory Standards Institute (CLSI), as described in the previous studies [44,45]. Briefly, the bacterial cells were incubated in Mueller–Hinton broth (MHB, Oxoid, Basingstoke, UK) at 37 °C and 150 rpm to the mid-growth phase and diluted to achieve a final concentration of 5 × 10<sup>5</sup> colony-forming units per milliliter (CFU/mL). Then, the cells were mixed with each peptide in different concentrations (1, 2, 4, 8, 16, 32, and 64 µg/mL). After co-incubation in MHB (150 rpm; 37 °C) for 16–20 h, the optical density at 630 nm (OD<sub>630</sub>) was determined, and the MIC value of each peptide was defined as the minimum peptide concentration with no detectable absorbance increase. All experiments were repeated at least three times.

#### 4.5. Hemolytic Activity Determination

The hemolytic activities of the peptides were determined against human red blood cells (hRBCs). As described [44], sodium citrate-anticoagulated hRBCs were washed three times with 0.9% sodium chloride and diluted to a final concentration of 4% (v/v). Then, an equal volume of hRBC solutions was mixed with an equal volume of each peptide in a series of concentrations (0, 2, 4, 8, 16, 32, 64, 128, 256, and 512 µg/mL). After co-incubation at 37 °C for 1 h, the degree of hemolysis of the peptides was determined by detecting the release of hemoglobin from the damaged hRBCs by measuring the optical density at 540 nm (OD<sub>540</sub>). hRBCs in 0.9% sodium chloride and 1% Triton X-100 were considered 0% and 100% hemolysis, respectively. The results shown are the average ± standard error of data derived from three independent experiments. The percent hemolysis was calculated according to the following equation [53,54]:

$$\text{Hemolysis (\%)} = 100 \times (A_{\text{sample}} - A_{\text{blank}}) / (A_{\text{positive}} - A_{\text{blank}})$$

#### 4.6. Growth Curve

The growth inhibitory effects of the peptides were measured against the standard strain *A. baumannii* ATCC19606 and the corresponding clinical isolates 19295, 19618, and 19462. Bacterial cells (5 × 10<sup>5</sup> CFU/mL) were incubated in MHB (150 rpm; 37 °C) without or with 0.25, 0.5, 1, 2, and 4 × MIC of the peptide for 9 h. At different time intervals, the OD<sub>630</sub> was measured to produce the curves of bacterial growth vs. time. The results are the average ± standard error of data derived from three independent experiments.

#### 4.7. Time-Killing Kinetics

Time-killing kinetics of the peptide were determined through the plate counting method. Briefly,  $2 \times 10^6$  CFU/mL bacterial cells were incubated in MHB at 150 rpm and 37 °C without or with the peptide at different concentrations (1, 2, and 4 × MIC). At each time interval (0, 5, 15, 30, and 60 min), aliquots were taken, and diluted serially, and 100 µL of the sample was spread on Mueller–Hinton agar. After overnight incubation, the surviving bacterial colonies of each plate were counted. The results are the average ± standard error of data derived from three independent experiments.

#### 4.8. Membrane Permeabilization Assay

Plasma membrane permeabilization of the bacterial cells caused by the peptide was determined by propidium iodide (PI, Thermo Fisher, Waltham, MA, USA) and SYTO™ Green (Thermo Fisher, Waltham, MA, USA) uptake assays, as described previously [25]. Briefly, exponential phase bacterial cells were collected by centrifugation ( $6000 \times g$ , 4 °C) and washed with phosphate-buffered saline (PBS). Next, the bacterial cells were diluted with PBS to achieve an absorbance of 0.1 at 630 nm and prepared in a sterile 96-well polypropylene plate. After mixing with 2 µM PI or 30 nM SYTO™ Green, a series dose of the peptide (1, 2, 4, and 8 × MIC) was added into each well, and fluorescence was immediately recorded on a Molecular Devices SpectraMax i3x (excitation wavelength: 535 nm for PI and 503 nm for SYTO™ Green; emission wavelength: 617 nm for PI and 530 nm for SYTO™ Green). All experiments were repeated at least three times. The results are the average ± standard error of data derived from three independent experiments.

**Supplementary Materials:** The following supporting information can be downloaded at: <https://www.mdpi.com/article/10.3390/toxins16030156/s1>, Figure S1: Correlations between net charge and hydrophobicity as well as hydrophobic moments of Ctriporin and its analogs.

**Author Contributions:** Conceptualization, Z.C. and X.L.; Data curation, X.L. and H.D.; Formal analysis, X.Y.; Investigation, X.L. and H.D.; Methodology, X.L.; Resources, L.D.; Software, X.Y.; Validation, F.S. and C.Q.; Funding Acquisition: Z.C. and X.L.; Supervision, Z.C.; Writing—original draft, X.L.; Writing—review & editing, Z.C. All authors have read and agreed to the published version of the manuscript.

**Funding:** This work was supported by grants from the Natural Science Foundation of Hubei Province (no. 2021CFB130), the School Natural Science Fund of Hubei University of Medicine (no. 2017QD-JZR14 and FDFR201906), and the National Natural Sciences Foundation of China (no. 81973321).

**Institutional Review Board Statement:** Hemolytic activity determination was conducted according to the guidelines of the Human Welfare and Research Ethics Committee of Hubei University of Medicine.

**Informed Consent Statement:** Informed consent was obtained from all subjects involved in the study.

**Data Availability Statement:** The data used and/or analyzed during the current study is available from the corresponding author on reasonable request.

**Conflicts of Interest:** The authors declare no conflicts of interest.

## References

1. Pendleton, J.N.; Gorman, S.P.; Gilmore, B.F. Clinical relevance of the ESKAPE pathogens. *Expert Rev. Anti. Infect. Ther.* **2013**, *11*, 297–308. [[CrossRef](#)]
2. Hu, F.; Zhu, D.; Wang, F.; Wang, M. Current status and trends of antibacterial resistance in China. *Clin. Infect. Dis.* **2018**, *67* (Suppl. S2), S128–S134. [[CrossRef](#)]
3. Oliveira, D.M.P.D.; Forde, B.M.; Kidd, T.J.; Harris, P.N.A.; Schembri, M.A.; Beatson, S.A.; Paterson, D.L.; Walkera, M.J. Antimicrobial resistance in ESKAPE pathogens. *Clin. Microbiol. Rev.* **2020**, *33*, e00181-19. [[CrossRef](#)]
4. Harrison, P.L.; Abdel-Rahman, M.A.; Miller, K.; Strong, P.N. Antimicrobial peptides from scorpion venoms. *Toxicon* **2014**, *88*, 115–137. [[CrossRef](#)] [[PubMed](#)]
5. Mylonakis, E.; Podsiadlowski, L.; Muhammed, M.; Vilcinskas, A. Diversity, evolution and medical applications of insect antimicrobial peptides. *Philos. Trans. R. Soc. Lond. B Biol. Sci.* **2016**, *371*, 20150290. [[CrossRef](#)] [[PubMed](#)]

6. Ladram, A.; Nicolas, P. Antimicrobial peptides from frog skin: Biodiversity and therapeutic promises. *Front. Biosci.* **2016**, *21*, 1341–1371. [[CrossRef](#)] [[PubMed](#)]
7. de Barros, E.; Goncalves, R.M.; Cardoso, M.H.; Santos, N.C.; Franco, O.L.; Candido, E.S. Snake venom cathelicidins as natural antimicrobial peptides. *Front. Pharmacol.* **2019**, *10*, 1415. [[CrossRef](#)] [[PubMed](#)]
8. D'Andrea, L.D.; Romanelli, A. Temporins: Multifunctional peptides from frog skin. *Int. J. Mol. Sci.* **2023**, *24*, 5426. [[CrossRef](#)] [[PubMed](#)]
9. Rincón-Cortés, C.A.; Bayona-Rojas, M.A.; Reyes-Montaña, E.A.; Vega-Castro, N.A. Antimicrobial activity developed by scorpion venoms and its peptide component. *Toxins* **2022**, *14*, 740. [[CrossRef](#)]
10. Ciumac, D.; Gong, H.; Hu, X.; Lu, J.R. Membrane targeting cationic antimicrobial peptides. *J. Colloid Interface Sci.* **2019**, *537*, 163–185. [[CrossRef](#)]
11. Lee, T.H.; Hall, K.N.; Aguilar, M.I. Antimicrobial peptide structure and mechanism of action: A focus on the role of membrane structure. *Curr. Top. Med. Chem.* **2016**, *16*, 25–39. [[CrossRef](#)] [[PubMed](#)]
12. Mahlapuu, M.; Hakansson, J.; Ringstad, L.; Bjorn, C. Antimicrobial peptides: An emerging category of therapeutic agents. *Front. Cell. Infect. Microbiol.* **2016**, *6*, 194. [[CrossRef](#)] [[PubMed](#)]
13. Kmeck, A.; Tancer, R.J.; Ventura, C.R.; Wiedman, G.R. Synergies with and resistance to membrane-active peptides. *Antibiotics* **2020**, *9*, 620. [[CrossRef](#)] [[PubMed](#)]
14. Ghosh, C.; Sarkar, P.; Issa, R.; Haldar, J. Alternatives to conventional antibiotics in the era of antimicrobial resistance. *Trends Microbiol.* **2019**, *27*, 323–338. [[CrossRef](#)] [[PubMed](#)]
15. Rodriguez de la Vega, R.C.; Schwartz, E.F.; Possani, L.D. Mining on scorpion venom biodiversity. *Toxicon* **2010**, *56*, 1155–1161. [[CrossRef](#)]
16. Ortiz, E.; Gurrola, G.B.; Schwartz, E.F.; Possani, L.D. Scorpion venom components as potential candidates for drug development. *Toxicon* **2015**, *93*, 125–135. [[CrossRef](#)]
17. Fan, Z.; Cao, L.; He, Y.; Hu, J.; Di, Z.; Wu, Y.; Li, W.; Cao, Z. Ctriporin, a new anti-methicillin-resistant *Staphylococcus aureus* peptide from the venom of the scorpion *Chaerilus tricostratus*. *Antimicrob. Agents Chemother.* **2011**, *55*, 5220–5229. [[CrossRef](#)]
18. Dai, C.; Ma, Y.; Zhao, Z.; Zhao, R.; Wang, Q.; Wu, Y.; Cao, Z.; Li, W. Mucroporin, the first cationic host defense peptide from the venom of *Lychas mucronatus*. *Antimicrob. Agents Chemother.* **2008**, *52*, 3967–3972. [[CrossRef](#)]
19. Zhao, Z.H.; Ma, Y.B.; Dai, C.; Zhao, R.M.; Li, S.R.; Wu, Y.L.; Cao, Z.J.; Li, W.X. Imcroporin, a new cationic antimicrobial peptide from the venom of the scorpion *Isometrus maculatus*. *Antimicrob. Agents Chemother.* **2009**, *53*, 3472–3477. [[CrossRef](#)]
20. de Melo, E.T.; Estrela, A.B.; Santos, E.C.; Machado, P.R.; Farias, K.J.; Torres, T.M.; Carvalho, E.; Lima, J.P.; Silva-Junior, A.A.; Barbosa, E.G.; et al. Structural characterization of a novel peptide with antimicrobial activity from the venom gland of the scorpion *Tityus stigmurus*: Stigmurin. *Peptides* **2015**, *68*, 3–10. [[CrossRef](#)]
21. Guo, X.; Ma, C.; Du, Q.; Wei, R.; Wang, L.; Zhou, M.; Chen, T.; Shaw, C. Two peptides, TsAP-1 and TsAP-2, from the venom of the Brazilian yellow scorpion, *Tityus serrulatus*: Evaluation of their antimicrobial and anticancer activities. *Biochimie* **2013**, *95*, 1784–1794. [[CrossRef](#)]
22. Almaaytah, A.; Zhou, M.; Wang, L.; Chen, T.; Walker, B.; Shaw, C. Antimicrobial/cytolytic peptides from the venom of the North African scorpion, *Androctonus amoreuxi*: Biochemical and functional characterization of natural peptides and a single site-substituted analog. *Peptides* **2012**, *35*, 291–299. [[CrossRef](#)]
23. Luo, F.; Zeng, X.C.; Hahin, R.; Cao, Z.J.; Liu, H.; Li, W.X. Genomic organization of four novel nondisulfide-bridged peptides from scorpion *Mesobuthus martensii* Karsch: Gaining insight into evolutionary mechanism. *Peptides* **2005**, *26*, 2427–2433. [[CrossRef](#)]
24. Zhao, Z.; Zhang, K.; Zhu, W.; Ye, X.; Ding, L.; Jiang, H.; Li, F.; Chen, Z.; Luo, X. Two new cationic  $\alpha$ -helical peptides identified from the venom gland of *Liocheles australasiae* possess antimicrobial activity against methicillin-resistant staphylococci. *Toxicon* **2021**, *196*, 63–73. [[CrossRef](#)]
25. Luo, X.; Ye, X.; Ding, L.; Zhu, W.; Zhao, Z.; Luo, D.; Liu, N.; Sun, L.; Chen, Z. Identification of the scorpion venom-derived antimicrobial peptide Hp1404 as a new antimicrobial agent against carbapenem-resistant *Acinetobacter baumannii*. *Microb. Pathog.* **2021**, *157*, 104960. [[CrossRef](#)] [[PubMed](#)]
26. Gautier, R.; Douguet, D.; Antonny, B.; Drin, G. HELIQUEST: A web server to screen sequences with specific  $\alpha$ -helical properties. *Bioinformatics* **2008**, *24*, 2101–2102. [[CrossRef](#)] [[PubMed](#)]
27. Rodriguez, A.; Villegas, E.; Satake, H.; Possani, L.D.; Corzo, G. Amino acid substitutions in an  $\alpha$ -helical antimicrobial arachnid peptide affect its chemical properties and biological activity towards pathogenic bacteria but improves its therapeutic index. *Amino Acids* **2011**, *40*, 61–68. [[CrossRef](#)] [[PubMed](#)]
28. Wiegand, I.; Hilpert, K.; Hancock, R.E. Agar and broth dilution methods to determine the minimal inhibitory concentration (MIC) of antimicrobial substances. *Nat. Protoc.* **2008**, *3*, 163–175. [[CrossRef](#)] [[PubMed](#)]
29. Torres, M.D.T.; Sothiselvam, S.; Lu, T.K.; de la Fuente-Nunez, C. Peptide design principles for antimicrobial applications. *J. Mol. Biol.* **2019**, *431*, 3547–3567. [[CrossRef](#)] [[PubMed](#)]
30. Liu, K.; Shao, W.M.; Chen, G.M. Autoencoder-based nonlinear Bayesian locally weighted regression for soft sensor development. *ISA Trans.* **2020**, *103*, 143–155. [[CrossRef](#)]
31. Karl, A.S.; Steel, J.G.; Warr, G.B. Regression fitting megavoltage depth dose curves to determine material relative electron density in radiotherapy. *Phys. Eng. Sci. Med.* **2023**, *46*, 1387–1397. [[CrossRef](#)] [[PubMed](#)]
32. Wilyard, C. The drug-resistant bacteria that pose the greatest health threats. *Nature* **2017**, *543*, 15. [[CrossRef](#)] [[PubMed](#)]

33. Liu, G.; Yang, F.; Li, F.; Li, Z.; Lang, Y.; Shen, B.; Wu, Y.; Li, W.; Harrison, P.L.; Strong, P.N.; et al. Therapeutic potential of a scorpion venom-derived antimicrobial peptide and its homologs against antibiotic-resistant gram-positive bacteria. *Front. Microbiol.* **2018**, *9*, 1159. [[CrossRef](#)] [[PubMed](#)]
34. Mishra, B.; Lakshmaiah Narayana, J.; Lushnikova, T.; Wang, X.; Wang, G. Low cationicity is important for systemic in vivo efficacy of database-derived peptides against drug-resistant gram-positive pathogens. *Proc. Natl. Acad. Sci. USA* **2019**, *116*, 13517–13522. [[CrossRef](#)] [[PubMed](#)]
35. Wang, G.; Li, X.; Wang, Z. APD3: The antimicrobial peptide database as a tool for research and education. *Nucleic Acids Res.* **2016**, *44*, D1087–D1093. [[CrossRef](#)] [[PubMed](#)]
36. Zhou, J.J.; Zhang, L.S.; He, Y.H.; Liu, K.X.; Zhang, F.F.; Zhang, H.R.; Lu, Y.Q.; Yang, C.Y.; Wang, Z.P.; Fareed, M.S.; et al. An optimized analog of antimicrobial peptide Jelleine-1 shows enhanced antimicrobial activity against multidrug resistant and negligible toxicity in vitro and in vivo. *Eur. J. Med. Chem.* **2021**, *219*, 113433. [[CrossRef](#)] [[PubMed](#)]
37. Liscano, Y.; Salamanca, C.H.; Vargas, L.; Cantor, S.; Laverde-Rojas, V.; Oñate-Garzón, J. Increases in hydrophilicity and charge on the polar face of alyteserin 1c helix change its selectivity towards gram-positive bacteria. *Antibiotics* **2019**, *8*, 238. [[CrossRef](#)]
38. Mourtada, R.; Herce, H.D.; Yin, D.J.; Moroco, J.A.; Wales, T.E.; Engen, J.R.; Walensky, L.D. Design of stapled antimicrobial peptides that are stable, nontoxic and kill antibiotic-resistant bacteria in mice. *Nat. Biotechnol.* **2019**, *37*, 1186–1197. [[CrossRef](#)]
39. Jiang, M.; Yang, X.; Wu, H.; Huang, Y.; Dou, J.; Zhou, C.; Ma, L. An active domain HF-18 derived from hagfish intestinal peptide effectively inhibited drug-resistant bacteria in vitro/vivo. *Biochem. Pharmacol.* **2020**, *172*, 113746. [[CrossRef](#)]
40. Stone, T.A.; Cole, G.B.; Ravamehr-Lake, D.; Nguyen, H.Q.; Khan, F.; Sharpe, S.; Deber, C.M. Positive charge patterning and hydrophobicity of membrane-active antimicrobial peptides as determinants of activity, toxicity, and pharmacokinetic stability. *J. Med. Chem.* **2019**, *62*, 6276–6286. [[CrossRef](#)]
41. Tan, Y.N.; Chen, X.L.; Ma, C.B.; Xi, X.P.; Wang, L.; Zhou, M.; Burrows, J.F.; Kwok, H.F.; Chen, T.B. Biological activities of cationicity-enhanced and hydrophobicity-optimized analogues of an antimicrobial peptide, dermaseptin-ps3, from the skin secretion of *Phyllomedusa sauvaagii*. *Toxins* **2018**, *10*, 320. [[CrossRef](#)]
42. Pedron, C.N.; Torres, M.T.; Lima, J.; Silva, P.I.; Silva, F.D.; Oliveira, V.X. Novel designed VmCT1 analogs with increased antimicrobial activity. *Eur. J. Med. Chem.* **2017**, *126*, 456–463. [[CrossRef](#)]
43. Oliveira, C.S.; Torres, M.T.; Pedron, C.N.; Andrade, V.B.; Silva, P.I., Jr.; Silva, F.D.; de la Fuente-Nunez, C.; Oliveira, V.X., Jr. Synthetic peptide derived from scorpion venom displays minimal toxicity and anti-infective activity in an animal model. *ACS Infect. Dis.* **2021**, *7*, 2736–2745. [[CrossRef](#)] [[PubMed](#)]
44. Luo, X.; Ye, X.; Ding, L.; Zhu, W.; Yi, P.; Zhao, Z.; Gao, H.; Shu, Z.; Li, S.; Sang, M.; et al. Fine-tuning of alkaline residues on the hydrophilic face provides a non-toxic cationic alpha-helical antimicrobial peptide against antibiotic-resistant ESKAPE pathogens. *Front. Microbiol.* **2021**, *12*, 684591.
45. Cao, L.; Dai, C.; Li, Z.; Fan, Z.; Song, Y.; Wu, Y.; Cao, Z.; Li, W. Antibacterial activity and mechanism of a scorpion venom peptide derivative in vitro and in vivo. *PLoS ONE* **2012**, *7*, e40135. [[CrossRef](#)] [[PubMed](#)]
46. Jiang, Z.; Vasil, A.I.; Hale, J.D.; Hancock, R.E.; Vasil, M.L.; Hodges, R.S. Effects of net charge and the number of positively charged residues on the biological activity of amphipathic  $\alpha$ -helical cationic antimicrobial peptides. *Biopolymers* **2008**, *90*, 369–383. [[CrossRef](#)] [[PubMed](#)]
47. Cao, L.; Li, Z.; Zhang, R.; Wu, Y.; Li, W.; Cao, Z. StCT2, a new antibacterial peptide characterized from the venom of the scorpion *Scorpiops tibetanus*. *Peptides* **2012**, *36*, 213–220. [[CrossRef](#)] [[PubMed](#)]
48. Zeng, X.C.; Zhou, L.; Shi, W.; Luo, X.; Zhang, L.; Nie, Y.; Wang, J.; Wu, S.; Cao, B.; Cao, H. Three new antimicrobial peptides from the scorpion *Pandinus imperator*. *Peptides* **2013**, *45*, 28–34. [[CrossRef](#)] [[PubMed](#)]
49. Li, Z.; Xu, X.; Meng, L.; Zhang, Q.; Cao, L.; Li, W.; Wu, Y.; Cao, Z. Hp1404, a new antimicrobial peptide from the scorpion *Heterometrus petersii*. *PLoS ONE* **2014**, *9*, e97539. [[CrossRef](#)] [[PubMed](#)]
50. Acevedo, I.C.C.; Silva, P.I., Jr.; Silva, F.D.; Araujo, I.; Alves, F.L.; Oliveira, C.S.; Oliveira, V.X., Jr. IsCT-based analogs intending better biological activity. *J. Pept. Sci.* **2019**, *25*, e3219. [[CrossRef](#)]
51. Ding, L.; Hao, J.; Luo, X.; Zhu, W.; Wu, Z.; Qian, Y.; Hu, F.; Liu, T.; Ruan, X.; Li, S.; et al. The Kv1.3 channel-inhibitory toxin BF9 also displays anticoagulant activity via inhibition of factor XIa. *Toxicon* **2018**, *152*, 9–15. [[CrossRef](#)] [[PubMed](#)]
52. Saranathan, R.; Vasanth, V.; Vasanth, T.; Shabareesh, P.R.; Shashikala, P.; Devi, C.S.; Kalaivani, R.; Asir, J.; Sudhakar, P.; Prashanth, K. Emergence of carbapenem non-susceptible multidrug resistant *Acinetobacter baumannii* strains of clonal complexes 103(B) and 92(B) harboring OXA-type carbapenemases and metallo- $\beta$ -lactamases in Southern India. *Microbiol. Immunol.* **2015**, *59*, 277–284. [[CrossRef](#)] [[PubMed](#)]
53. Yin, L.M.; Edwards, M.A.; Li, J.; Yip, C.M.; Deber, C.M. Roles of hydrophobicity and charge distribution of cationic antimicrobial peptides in peptide-membrane interactions. *J. Biol. Chem.* **2012**, *287*, 7738–7745. [[CrossRef](#)] [[PubMed](#)]
54. Li, Z.; Liu, G.; Meng, L.; Yu, W.; Xu, X.; Li, W.; Wu, Y.; Cao, Z. K1K8: An Hp1404-derived antibacterial peptide. *Appl. Microbiol. Biotechnol.* **2016**, *100*, 5069–5077. [[CrossRef](#)]

**Disclaimer/Publisher’s Note:** The statements, opinions and data contained in all publications are solely those of the individual author(s) and contributor(s) and not of MDPI and/or the editor(s). MDPI and/or the editor(s) disclaim responsibility for any injury to people or property resulting from any ideas, methods, instructions or products referred to in the content.